Symmetry-adapted linear combination of atomic orbitals bases and band-structure computation for quasi-one-dimensional solids

Ivan Božović*
Department of Physics, University of California, Berkeley, California 94720

Joseph Delhalle
Laboratoire de Chimie Théorique Appliquée, Facultés Universitaires Notre-Dame de la Paix, 61 rue de Bruxelles, B-5000 Namur, Belgium

(Received 25 July 1983)

A method to derive LCAO bases adapted to the symmetry of a quasi-one-dimensional crystal is presented. The complete solution is given for chains of $L(2q)_q mc$ line-group symmetry in general and for the beryllium hydride polymer and tetracyanoplatinate chain in particular. We also give a quantitative account of computational reductions and discuss band touchings and slopes, crystal-field splitting, and selection rules for direct optical absorption.

I. INTRODUCTION

Discoveries of pyroelectric and piezoelectric (polyvinylidene fluoride), photoconducting (polyvinyl carbazole, etc.), conducting [polyacetylene, polyparaphenylene, tetrathiafulvalene-tetracyanoquinodimethane, (TTF-TCNQ), potassium tetracyanoplatinate complexes (KCP), etc.] and superconducting [polysulfur nitride, $NbSe_3$, bis-tetramethyltetraselenafulvalene perchlorate $(TMTSF)_2ClO_4$, etc.] polymers and quasi-one-dimensional (quasi-1D) solids have stimulated extensive investigation on their electronic properties.[1] One-electron band-structure computations on model chains,[2] ranging from semiempirical to *ab initio* Hartree-Fock, provide information on charge-density distributions, geometric structure and force constants (via potential energy surface scanning), charge-carrier mobilities along the chain, etc. Offering a conceptual framework for interpretation of related experimental [x-ray photoelectron spectroscopy (XPS), electron energy-loss spectroscopy (EELS), etc.] data, they contribute to our understanding of structure and properties of these materials. In this paper, we implant explicit symmetry considerations into such computations, trying to improve their efficiency and obtain additional physical insight.

Polymers and quasi-1D solids possess specific spatial symmetries, properly described in terms of *line groups*.[3,4] Utilizing the analogy with the crystallographic space groups as much as possible, we could express most of line-group theoretical results in terms already familiar to a solid-state physicist (Brillouin zone, band and star degeneracies, compatibility, etc). Motivation for independent study of the line groups stems from their advantageous structural features (uniaxial rotations, order-2 subgroup chains, comprehension of a whole infinite family of line groups by a single parametrized formula, etc. (cf. Sec. II), enabling us to complete certain tasks [e.g., to tabulate symmetry-adapted bases (SAB's)] that would be very impractical to perform for all the three-dimensional (3D) 230 space groups. Next, it is possible to give a clear physical interpretation (quasimomentum, quasi-angular-momentum, mirror-plane parities, etc.) of the quantum numbers arising from the line groups, and thus to express our results in very simple terms, avoiding elaborate group-theoretical parlance. Finally, in 3D crystals, general $\vec{k}$ vectors outnumber the special $\vec{k}$ vectors (viz., those that are invariant under some symmetry operations); in contrast, for all but a few of the most trivial line groups, *every* k point is a special point; thereby importance of symmetry considerations is greatly enhanced in the case of chainlike systems. However, apart from the translational symmetry and the simplest (cyclic) line groups,[5] only a few other line groups were considered[6]; therefore a systematic study of all line groups has been undertaken,[4,7,8] this paper comprising the part devoted to the applications of line-group theory to linear combination of atomic orbitals (LCAO) band-structure calculations on polymers.

The paper is organized as follows. The method we use to derive the LCAO SAB's is expounded in Sec. II and illustrated in the Appendix, where such a basis is explicitly tabulated for the $L(2q)_q mc$ line groups, the most complex within this approach. The form of one-electron equations in the new basis is discussed, and a quantitative account is given for the computational reductions (in the format of matrices and in the number of integrals). For many quasi-1D and polymeric conductors the line-group symmetry is specified, and two examples—beryllium hydride polymer and tetracyanoplatinate chain, both of great interest by themselves[9,10]—are considered in detail (SAB's, equations, computational savings, band-structure features, compatibility, selection rules, crystal-field splitting) in Secs. III and IV, respectively.

II. LINE-GROUP SYMMETRY-ADAPTED LCAO'S AND BAND-STRUCTURE COMPUTATIONS

A. Line groups

The spatial symmetry groups of physical systems periodic along a line—such as stereoregular polymers and

TABLE I. Line groups and their isogonal point groups. Here $n=1,2,\ldots$, $p=0,1,\ldots,n-1$, and $q=n/2=1,2,\ldots$. $\hat{C}_n$, $\hat{\sigma}_v$, $\hat{\sigma}_h$, and $\hat{U}$ are defined in the text (in Sec. II A) and $\hat{U}_d=\hat{C}_{2n}\hat{U}$. The relevant index-2 subgroup structure of the line groups is explicitly shown below.

Point group	Line group: n odd	Line group: n even
C_n	Ln Ln_p	
C_{nv}	$Lnm=Ln+(\hat{\sigma}_v\mid 0)Ln$ $Lnc=Ln+(\hat{\sigma}_v\mid \frac{1}{2})Ln$	$Lnmm=Ln+(\hat{\sigma}_v\mid 0)Ln$ $Lncc=Ln+(\hat{\sigma}_v\mid \frac{1}{2})Ln$ $L(2q)_qmc=L(2q)_q+(\hat{\sigma}_v\mid 0)L(2q)_q$
C_{nh}	$Ln/m=Ln+(\hat{\sigma}_h\mid 0)Ln$ $L(2q)_q/m=L(2q)_q+(\hat{\sigma}_h\mid 0)L(2q)_q$	
S_{2n}	$L\bar{n}=Ln+(\hat{\sigma}_h\hat{C}_{2n}\mid 0)Ln$	$L(\bar{2n})=Ln+(\hat{\sigma}_h\hat{C}_{2n}\mid 0)Ln$
D_n	$Ln2=Ln+(\hat{U}\mid 0)Ln$ $Ln_p2=Ln_p+(\hat{U}\mid 0)Ln_p$	$Ln22=Ln+(\hat{U}\mid 0)Ln$ $Ln_p22=Ln_p+(\hat{U}\mid 0)Ln_p$
D_{nd}	$L\bar{n}m=Lnm+(\hat{U}_d\mid 0)Lnm$ $L\bar{n}c=Lnc+(\hat{U}_d\mid 0)Lnc$	$L(\bar{2n})2m=Lnmm+(\hat{U}_d\mid 0)Lnmm$ $L(\bar{2n})2c=Lncc+(\hat{U}_d\mid 0)Lncc$
D_{nh}	$L(\bar{2n})2m=Lnm+(\hat{\sigma}_h\mid 0)Lnm$ $L(\bar{2n})2c=Lnc+(\hat{\sigma}_h\mid 0)Lnc$	$Ln/mmm=Lnmm+(\hat{\sigma}_h\mid 0)Lnmm$ $Ln/mcc=Lncc+(\hat{\sigma}_h\mid 0)Lncc$ $L(2q)_q/mcm=L(2q)_qmc+(\hat{\sigma}_h\mid 0)L(2q)_qmc$
$C_{\infty v}$	$L\infty m$	
$D_{\infty h}$	$L\infty/mm=L\infty m+(\hat{\sigma}_h\mid 0)L\infty m$	

atomic chains or molecular stacks in quasi-1D solids—are line groups.[3,4] [Line groups are frequently confused with either strip (*Streiffen*) groups or one-dimensional space groups; in fact, they correspond to arrays of three-, two-, and one-dimensional objects, respectively.]

Let $(\hat{R}\mid\tau)$ denote an element of a line group L; if the z axis coincides with the chain axis, then $(\hat{R}\mid\tau)\vec{r}=\hat{R}\vec{r}+\tau a\vec{e}_z$, where a is the translational period, $\tau=t+v$, where $0\le v<1$ and $t=0,\pm1,\pm2,\ldots$. $\hat{R}=\hat{C}_n$, $\hat{\sigma}_v$, $\hat{\sigma}_h$, $\hat{U}$, or a combination of these transformations. Here $\hat{C}_n$ denotes a rotation through $\alpha=2\pi/n$ around the z axis; n may be any integer so that the number of line groups is unlimited. (There are 75 crystallographic line groups in which $n=1$, 2, 3, 4 or 6; they appear as proper subgroups in the space groups. However, for a single chain one frequently finds $n=5$, 7, etc.; in some polymers $n\ge40$.) The mirror reflections in the xz and the xy planes are denoted by $\hat{\sigma}_v$ and $\hat{\sigma}_h$, respectively, and $\hat{U}$ is the rotation through $\alpha=\pi$ around the x axis. A line group is denoted, in the international crystallographic (Hermann-Mauguin) manner, by Ln_p ($p=0,1,\ldots,n-1$) if it contains a screw axis $(\hat{C}_n\mid p/n)$, by Ln_p2 if it also contains $(\hat{U}\mid 0)$, etc. The list of all line groups (with relevant subgroup structure indicated) is given in Table I, and some of currently most interesting chain compounds are classified according to their line-group symmetry in Fig. 1 and Table II.

With translational symmetry, it is sufficient to consider explicitly one unit cell instead of the whole periodic ob-

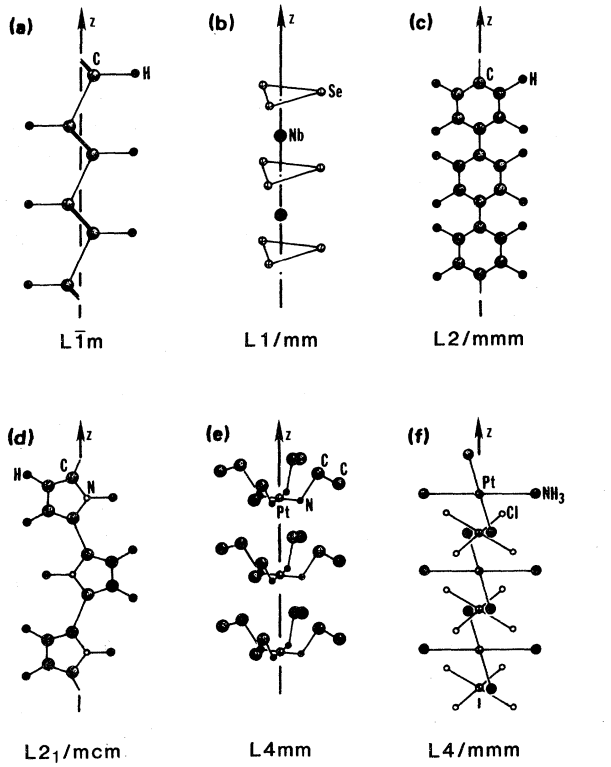

FIG. 1. Examples of line-group symmetries of polymers and quasi-1D molecular stacks. (a) *trans*-polyacetylene, (b) $NbSe_3$, (c) planar (polyparaphenylene), (d) polypyrrole, (e) Wolfram's red salt, (f) Magnus's green salt.

TABLE II. List of some representative quasi-1D conductors, molecular stacks, and polymers, classified according to line-group symmetry. The following definitions apply: TMTSF, bis-tetramethyltetraselenafulvalene; NMP, *N*-methylphenazinium; HMTTF, hexamethylenetetrathiafulvalene; TTT, tetrathiatetracene; TSeT, tetraselenatetracene.

Line group	Compounds
$L\bar{1}m$	*trans*-polyacetylene or *trans*-$(CH)_x$, poly(*p*-phenylene sulfide) or $(C_6H_4^-S^-)_x$, TMTSF–,NMP–, HMTTF– stacks
$L\,1/mm$	MX_3 (M=Nb,Ti,Zr,Ta; X=S,Se,Te) chains
$L\,2_1mc$	polysulfurnitride or $(SN)_x$
$L\,2/mcc$	poly(*p*-phenylene) or $(C_6H_4)_x$
$L\,2/mmm$	tetracyanoquinodimethane (TCNQ) stacks, tetrathiafulvalene (TTF) stacks, planar poly(*p*-phenylene)
$L\,2_1/mcm$	TTT stacks, TSeT stacks, *cistransoid*- and *transcisoid*-polyacetylene, poly(pyrrole)
$L\,4mm$	Wolfram's red salts, e.g., $[Pt(ea)_4][Pt(ea)_4Br_2]Br_4$ (ea=ethylamine)
$L\,4/mmm$	Magnus's green salts, e.g., $PtCl_4PtN_4$, porphyrinic molecular metals
$L\,4_2/mcm$	beryllium hydride or $(BeH_2)_x$, beryllium chloride or $(BeCl_2)_x$
$L\,8_4/mcm$	$K_2Pt(CN)_4$

ject. Additional symmetries (rotation and screw axes, mirror and glide planes) further decrease the relevant portion (asymmetric unit) of the polymer onto a *basic motif,* i.e., the minimal part from which the line group recovers the rest.

B. Irreducible representation and SAB's of line groups

Let V be a state space [spanned by the initial set of atomic orbitals (AO's)] and let

$$\hat{P}_{ij}^{\alpha}=\frac{d_\alpha}{|L|}\sum_{(\hat{R}\,|\,\tau)\in L}\hat{D}_{ij}(\hat{R}\,|\,\tau)^*[\hat{R}\,|\,\tau]\,, \tag{1}$$

where $\underline{D}^{\alpha}$ is a unitary irreducible representation (irrep) of the corresponding line group L, d_α is the dimension of $\underline{D}^{\alpha}$, $|L|$ is the order of L (assumed finite in virtue of the Born–von Kármán periodic boundary conditions), and $[\hat{R}\,|\,\tau]$ is a (reducible) unitary operator defined in V by

$$[\hat{R}\,|\,\tau]\Phi(\vec{r})\equiv\Phi((\hat{R}\,|\,\tau)^{-1}\vec{r})\,.$$

Utilizing $\hat{P}_{ij}^{\alpha}$ one can construct a basis of V, symmetry-adapted (SAB) with respect to L, according to the well-known[11] algorithm: (i) specify the input data (atomic positions, orbitals, irreps $\underline{D}^{\alpha}$), (ii) determine the matrices of $[\hat{R}\,|\,\tau]$ for each $(\hat{R}\,|\,\tau)\in L$, (iii) form $\hat{P}_{ii}^{\alpha}$, $i=1,\ldots,d_\alpha$, (iv) apply them to obtain symmetry-adapted columns, and (v) select from these a linearly independent set. (For the space groups, a computer routine has been developed[12] along these lines; the required irreps are generated each time.) The question we posed ourselves was, is it possible to perform this task only once by tabulating ready-to-use line-group LCAO SAB's—or even better, by writing the final one-electron (extended-Hückel, pseudopotential, etc.) equations in a symmetry-adapted form? The answer is positive, due to the following observations. First, the irreps $\underline{D}^{\alpha}$ of all the line groups are now available[7] (in a parametrized form). Second, the action of $[\hat{R}\,|\,\tau]$ onto an AO $\Phi(\vec{r}-\vec{R}_u)$ consists of an on-site transformation (rotation and/or reflection) $\hat{R}\Phi(\vec{r})\rightarrow\tilde{\Phi}(\vec{r})$ followed by a site change $\vec{R}_u\rightarrow\vec{R}_v=(\hat{R}\,|\,\tau)\vec{R}_u$ so that altogether one has

$$[\hat{R}\,|\,\tau]\Phi(\vec{r}-\vec{R}_v)=\tilde{\Phi}(\vec{r}-\vec{R}_v)\,.$$

Each of these two mappings ($\Phi\rightarrow\tilde{\Phi}$ and $\vec{R}_u\rightarrow\vec{R}_v$) can be completely specified when an appropriate classification of AO's and atomic sites is made.

C. On-site transformations: Types of AO's

If the AO's are of the form

$$\Phi^{m_z}=f(r,\theta)e^{im_z\phi}\,,$$

a pair $\{\Phi^{m_z},\Phi^{-m_z}\}$ (with $m_z>0$) can be replaced by an equivalent pair $\{\Phi_+^{m_z},\Phi_-^{m_z}\}$ of real AO's defined by

$$\Phi_+^{m_z}=f(r,\theta)\cos(m_z\phi)$$

and

$$\Phi_-^{m_z}=f(r,\theta)\sin(m_z\phi)\,.$$

In this classification s, p_z, and d_{z^2} orbitals are of Φ^0 type, $\{p_x,p_y\}$ and $\{d_{xz},d_{yz}\}$ are pairs of $\{\Phi_+^1,\Phi_-^1\}$ type, $\{d_{x^2-y^2},d_{xy}\}$ is a pair of $\{\Phi_+^2,\Phi_-^2\}$ type, etc. One can easily verify that

$$\hat{C}_n^s\Phi^0=\Phi^0\,, \tag{2a}$$

$$\hat{C}_n^s\Phi_+^{m_z}=\cos(m_zs\alpha)\Phi_+^{m_z}+\sin(m_zs\alpha)\Phi_-^{m_z}\,, \tag{2b}$$

$$\hat{C}_n^s\Phi_-=-\sin(m_zs\alpha)\Phi_+^{m_z}+\cos(m_zs\alpha)\Phi_-^{m_z}\,, \tag{2c}$$

and

$$\hat{\sigma}_v\Phi^0=\Phi^0\,, \tag{3a}$$

$$\hat{\sigma}_v\Phi_\pm^{m_z}=\pm\Phi_\pm^{m_z}\,. \tag{3b}$$

D. Site permutations: Graphs of line groups

Any polymer can be viewed as the union of simple (monatomic) subchains, each generated by the action of the operations of the corresponding line group L onto one of the atoms in the basic motif. We call the set Γ of the atomic sites belonging to one subchain a *graph* of L.

Now, if $\vec{R}_u \in \Gamma$ then $(\hat{R} \mid \tau)\vec{R}_u = \vec{R}_v \in \Gamma$, so that $(\hat{R} \mid \tau)$ defines a permutation $u \rightarrow v = \Pi(u)$. Two graphs are inequivalent if they give rise to different permutations; for each line group there are no more than few distinct graphs that can be found by inspection (or by enumeration of some special homomorphisms of L).

Thus we can completely determine the action of $[\hat{R} \mid \tau]$ onto an atomic orbital $\Phi_\lambda^{m_z}$ if its type (specified by m_z and λ) and the graph Γ to which it belongs are given; then the remaining steps (iii)—(v) are readily performed. Our task is solved when we tabulate the LCAO SAB's for each L, $\underline{D}^\alpha$, Γ, λ, and m_z.

E. LCAO SAB tables: Usage

Comprehensive tables of the LCAO SAB's for the line groups have been derived as outlined above; for the sake of brevity we list (in the Appendix) only those corresponding to the $L(2q)_q mc$ family of line groups. This choice is made because (a) they are the most complex groups to be computer-implanted in our approach, (b) they contain rotation and screw axes, mirror and glide planes, and thus they contain the features of all others, and (c) the actual physical systems [beryllium hydride polymers, $Pt(CN)_4$ chains] we extensively deal with later in this paper (cf. Secs. III and IV) belong to this family. As for (a), the line groups isogonal to C_n or C_{nv} significantly contribute to numerical savings; the effect of additional $(\hat{\sigma}_h, \hat{U}, \hat{U}_d)$ symmetries is negligible and we use them *a posteriori* (via the compatibility relations, etc.; cf. Secs. III and IV). The relevant subgroup is indicated for each line group in Table I.

The graphs of $L(2q)_q mc$ are Γ_z containing points on the z axis (two points per translation period), Γ_v generated by a point in the σ_v plane ($2q$ points per period), and Γ_a with a generating point in an arbitrary asymmetric position ($4q$ points per period). The irreps of $L(2q)_q mc$ are one-dimensional (${}_kA_0$, ${}_kB_0$, ${}_kA_q$, ${}_kB_q$) and two-dimensional (${}_kE_{m,-m}$, $m = 1, \ldots, q-1$), the latter bringing in twofold band degeneracies; they are reproduced in Table III.

For each graph and each irrep, only those orbitals that give rise to linearly independent symmetry-adapted LCAO's are listed and projected. For a given polymer, the user must find the tabulated LCAO for each orbital of each atom in the basic motif, and together these LCAO's constitute a complete SAB; the procedure is illustrated on $(BeH_2)_x$ in Sec. III.

F. One-electron equations in the LCAO SAB formulation

For a broad class of one-electron Hamiltonians (including those appearing in frequently used tight-binding, extended-Hückel, pseudopotential, etc., schemes), one can prove commutation of $\vec{H}$ with the corresponding line group L and therefore with $\hat{P}^\alpha_{ij}$. [In the self-consistent-field (SCF) Hartree-Fock (HF) method one should, however, be aware of the "symmetry dilemma." Incorrect numerical cutoffs may also violate the symmetry, as has happened frequently in the literature.] The commutation with L is preserved if one neglects

$$| \langle \Phi_\mu(\vec{r} - \vec{R}_\mu) \mid \Phi_\nu(\vec{r} - \vec{R}_\nu) \rangle |$$

when it is less than δ, or when $|\vec{R}_\mu - \vec{R}_\nu| \geq d$, where δ, d are specified constants; including the long-range summations is even better. Thus one expands

$$\psi = \sum_{\alpha i} \psi_{\alpha i}, \quad \psi_{\alpha i} = \sum_{\nu=1}^{\omega} C_{i\nu}(\alpha) \hat{P}^\alpha_{ii} \Phi_\nu$$

(where the index ν enumerates the ω AO's in the basic domain) to obtain

$$\sum_\nu C_{i\nu}(\alpha)[H_{\mu\nu}(\alpha) - \epsilon(\alpha) S_{\mu\nu}(\alpha)] = 0 \tag{4}$$

for each irrep $\underline{D}^\alpha$ of L, where

$$\begin{aligned} S_{\mu\nu}(\alpha) &\equiv \langle \Phi_\mu, \hat{P}^\alpha_{11} \Phi_\nu \rangle , \\ H_{\mu\nu}(\alpha) &\equiv \langle \Phi_\mu \hat{H} \hat{P}^\alpha_{11} \Phi_\nu \rangle . \end{aligned} \tag{5}$$

Since $\hat{P}^\alpha_{11}$ and $\hat{P}^\alpha_{ii}$, $i = 2, \ldots, d_\alpha$ (d_α being the dimension of $\underline{D}^\alpha$) give rise to identical $S_{\mu\nu}(\alpha)$ [and $H_{\mu\nu}(\alpha)$], Eqs. (4) do not depend on i, therefore explaining the systematic d_α-fold degeneracy.

Numerical savings achieved via this basis transformation are significant. Before proceeding to their quantitative estimation let us just stress that the numerical coefficients $C_{i\nu}(\alpha)$ appearing in the symmetry-adapted LCAO's and in the expansion of the matrix elements (5) in terms of those over the initial AO's are indeed the same.

TABLE III. irreps of the line groups $L(2q)_q mc$, $q = 1, 2, \ldots$. Here $\kappa(\tau) = \exp(ik\tau a)$, $M(s) = \begin{pmatrix} \mu & 0 \\ 0 & \mu^* \end{pmatrix}$, $N(s) = \begin{pmatrix} 0 & \mu \\ \mu^* & 0 \end{pmatrix}$, where $\mu = \exp(ims\alpha)$ and $t = 0, \pm 1, \pm 2, \ldots$, $\alpha = \pi/q$, $r = 0, 1, \ldots, q-1$, $-\pi/a < k \leq \pi/a$, $m = 1, 2, \ldots, q-1$.

irrep	$(C_{2q}^{2r} \mid t)$	$(C_{2q}^{2r+1} \mid \frac{1}{2} + t)$	$(\sigma_v C_{2q}^{2r} \mid t)$	$(\sigma_v C_{2q}^{2r+1} \mid \frac{1}{2} + t)$
${}_kA_0$	$\kappa(t)$	$\kappa(\frac{1}{2} + t)$	$\kappa(t)$	$\kappa(\frac{1}{2} + t)$
${}_kA_q$	$\kappa(t)$	$-\kappa(\frac{1}{2} + t)$	$\kappa(t)$	$-\kappa(\frac{1}{2} + t)$
${}_kB_0$	$\kappa(t)$	$\kappa(\frac{1}{2} + t)$	$-\kappa(t)$	$-\kappa(\frac{1}{2} + t)$
${}_kB_q$	$\kappa(t)$	$-\kappa(\frac{1}{2} + t)$	$-\kappa(t)$	$\kappa(\frac{1}{2} + t)$
${}_kE_{m,-m}$	$\kappa(t)M(2r)$	$\kappa(\frac{1}{2} + t)M(2r+1)$	$\kappa(t)N(2r)$	$\kappa(\frac{1}{2} + t)N(2r+1)$

G. Computational advantages

The LCAO SAB formulation of the one-electron eigenproblem, Eq. (4), offers the following advantages: (i) the format of the matrices to be diagonalized is lowered, (ii) the number of integrals over AO's to be calculated is reduced, and (iii) the one-electron states emerge with symmetry labels, useful for logical control of the calculations and for subsequent physical interpretation of the results.

To make the argument quantitative, let us consider an arbitrary polymer of $L(2q)_q mc$ symmetry, with a orbitals of Φ^0 type and b AO pairs of $\{\Phi_+^{m_z},\Phi_-^{m_z}\}$ type on Γ_z graphs, $c+2d$ on Γ_v graphs, and $e+2f$ on Γ_a graphs, in the basic domain. Let us further classify the above-mentioned b pairs of orbitals at Γ_z into b_1 pairs with $m_z=hq$, b_2 pairs with $\mathrm{Fr}(m_z/q)=\frac{1}{2}$, and b_3 pairs for which $m_z=-m+(h+1)q$, where $h=0,\pm1,\ldots,$ and $\mathrm{Fr}(x)$ is the fractional part of x. (These three conditions are indeed complementary.) The irreps of the one-dimensional translation group T are defined by $d_k(\hat{E}\mid t)=\exp(ikta)$, where $-\pi/a<k\le\pi/a$; hence V splits into the orthogonal sum of subspaces $V(d_k)$ of dimension

$$\dim V(d_k)=2(a+b)+2q(c+2d)+4q(e+2f)\ . \tag{6}$$

In the LCAO SAB of $L(2q)_q mc$, as given in the Appendix, each $V(d_k)$ splits further into the orthogonal sum of subspaces $V({}_k\underline{D}^\alpha)$ of the following dimensions:

$$\begin{aligned}
&\dim V({}_kA_0)=\dim V({}_kA_q)=a+b_1+c+d+e+2f\ ,\\
&\dim V({}_kB_0)=\dim V({}_kB_q)=b_1+d+2f\ ,\\
&\dim V({}_kE_{m,-m})=\begin{cases}2b_2+c+2d+2e+4f, & m=q/2\\ 2b_3+c+2d+2e+4f, & m=-m_z+(h+1)q\\ c+2d+2e+4f, & m=m_z-hq,\end{cases}
\end{aligned} \tag{7}$$

where $h=0,\pm1,\ldots$; the three conditions on m in ${}_kE_{m,-m}$ are complementary and altogether $m=1,\ldots,q-1$ (cf. the Appendix). Hence $\underline{H}(k)$ and $\underline{S}(k)$ matrices are block-diagonalized from $\Omega\times\Omega$ to a sum of blocks, dimensions of which are given in (7). For beryllium hydride polymer (cf. Sec. III A) in the valence-orbital description, this amounts to reduction from 12×12 to 3×3 matrices and for $Pt(CN)_4$ chain (cf. Sec. IV A) from 84×84 to at most 10×10. Since diagonalization is usually the computational bottleneck (except for the SCF HF method), evidently some interesting, but as yet intractable, systems are now brought within reach by virtue of line group SAB's.

Let us discuss now reductions in the number of integrals [item (ii)] to be computed. Traditionally, one would calculate the overlap integrals

$$\begin{bmatrix}0 & t\\ \mu & \nu\end{bmatrix}\equiv\int\Phi_\mu(\vec{r}-\vec{R}_\mu)\Phi_\nu(\vec{r}-\vec{R}_\nu-ta\vec{e}_z)d\vec{r}$$

to form the $\Omega\times\Omega$ blocks $\underline{S}(k)$, $-\pi/a<k\le\pi/a$, where

$$S_{\mu\nu}(k)=\sum_t\exp(-ikta)\begin{bmatrix}0 & t\\ \mu & \nu\end{bmatrix}$$

and analogously for $\underline{H}(k)$. Instead, for each irrep $\underline{D}^\alpha$ of $L(2q)_q mc$ we form $\underline{S}(\alpha)$ according to (5a), utilizing only some of the integrals $\left(\begin{smallmatrix}0\\ \mu\end{smallmatrix}\middle|\begin{smallmatrix}t\\ \nu\end{smallmatrix}\right)$.

For a given Φ_ν^t, let Φ_ν^0 denote the orbital belonging to the zeroth basic motif (BM), such that $\Phi_\nu^t=[\hat{R}\mid\tau]\Phi_\nu^0$ for some $[\hat{R}\mid\tau]\in L(2q)_q mc$. It can be seen that we do not need $\left(\begin{smallmatrix}0\\ \mu\end{smallmatrix}\middle|\begin{smallmatrix}t\\ \nu\end{smallmatrix}\right)$ unless

(1) Φ_μ^0 belongs to BM,

(2) both Φ_μ^0 and Φ_ν^0 contribute to some V^α, i.e., $(\Phi_\mu^0,\hat{P}^\alpha\Phi_\nu^0)\equiv(\hat{P}^\alpha\Phi_\mu^0,\Phi_\nu^0)\neq0$, or

(3) $\mu\le\nu'$.

It is straightforward but space consuming to analyze in detail the effects of cases (1)–(3) in terms of $a,b,\ldots,f$ and $\underline{D}^\alpha$; let us rather note that case (1) plays the major role for atoms in asymmetric positions in contrast to case (2), which mostly affects those on Γ_z. Also, note that case (3) is more strict than the traditional $\mu\le\nu$. Altogether the savings are remarkable; some numerical illustrations can be found in Secs. III and IV.

In view of frequent misunderstandings we feel it necessary to stress also that the integrals to be actually calculated within the two methods are indeed *the same;* only the linear combinations made from them afterwards are different. This point may be easily understood upon inspection of the overlap matrix for $(BeH_2)_x$ in the $L\,4_2mc$ LCAO SAB, given in Table IV.

In the line-group SAB formulation, the eigenvalues and eigenstates of $\underline{H}$ emerge automatically assigned to irreps of L [item (iii)]. These labels convey physical information on which we concentrate in Secs. III and IV; in addition, they bring in some computational advantage in terms of logical controls of the calculated bands and states. In addition to checks of degeneracy, transformation properties, frequencies of irreps, and band touchings at the zone center and edges, these labels are helpful in the case where two or more bands come close together or cross ("band-indexing difficulties").[2] *A posteriori* symmetry analysis of the reported band structures of polymers shows that incorrect interpolations, incorrect interaction truncations, and other artificial violations of symmetry were frequently made.

TABLE IV. Overlap matrix for the $(BeH_2)_x$ polymer, expressed in the LCAO SAB of $L4_2mc$. $\underline{S}(A_0)$ block corresponds to the irrep ${}_kA_0$, $\underline{S}(A_2)$ to ${}_kA_2$, and $\underline{S}(E_1)$ to the first column of ${}_kE_{1,-1}$. $\gamma \equiv \exp(-ika/2)$ and $-\pi/a < k \leq \pi/a$.

Atomic orbitals

$\Phi_1^0 = 2s(Be_1)$, $\Phi_2^0 = 2p_z(Be_1)$, $\Phi_3^0 = 2p_x(Be_1)$, $\Phi_4^0 = 2p_y(Be_1)$, $\Phi_5^0 = 1s(H_1)$, $\Phi_6^0 = 1s(H_2)$,
$\Phi_7^0 = 2s(Be_2)$, $\Phi_8^0 = 2p_z(Be_2)$, $\Phi_9^0 = 2p_y(Be_2)$, $\Phi_{10}^0 = 2p_x(Be_2)$, $\Phi_{11}^0 = 1s(H_3)$, $\Phi_{12}^0 = 1s(H_4)$

Overlap matrices

Block 1

$$\underline{S}(A_0) = \begin{bmatrix} S_{11} & S_{12} & S_{15} \\ S_{12}^* & S_{22} & S_{25} \\ S_{15}^* & S_{25}^* & S_{55} \end{bmatrix}, \text{ where}$$

$$S_{\mu,\nu} = \tfrac{1}{2}\sum_t \exp(-ikta)\left[\begin{bmatrix} 0 & t \\ \mu & \nu \end{bmatrix} + \gamma \begin{bmatrix} 0 & t \\ \mu & \nu+6 \end{bmatrix}\right], \quad \mu = 1,2, \quad \nu = 1,2,5, \ \mu \leq \nu \text{ and}$$

$$S_{5,5} = \tfrac{1}{4}\sum \exp(-ikta)\left[\begin{bmatrix} 0 & t \\ 5 & 5 \end{bmatrix} + \begin{bmatrix} 0 & t \\ 5 & 6 \end{bmatrix} + 2\gamma \begin{bmatrix} 0 & t \\ 5 & 11 \end{bmatrix}\right]$$

Block 2

$\underline{S}(A_2)$: same as $\underline{S}(A_0)$ but replace γ by $-\gamma$

Block 3

$$\underline{S}(E_1) = \begin{bmatrix} P_{33} & 0 & P_{35} \\ 0 & P_{33} & 0 \\ P_{35}^* & 0 & P_{55} \end{bmatrix}, \text{ where}$$

$$P_{3\nu} = \tfrac{1}{2}\sum \exp(-ikta)\left[\begin{bmatrix} 0 & t \\ 3 & \nu \end{bmatrix} - i\gamma \begin{bmatrix} 0 & t \\ 3 & \nu+6 \end{bmatrix}\right], \quad \nu = 3,5 \text{ and}$$

$$P_{55} = \tfrac{1}{2}\sum \exp(-ikta)\left[\begin{bmatrix} 0 & t \\ 5 & 5 \end{bmatrix} - \begin{bmatrix} 0 & t \\ 5 & 6 \end{bmatrix}\right]$$

III. EXAMPLE: BAND STRUCTURE OF BERYLLIUM HYDRIDE POLYMER

A. Symmetry-adapted one-electron eigenproblem

The translational repeat unit of the $(BeH_2)_x$ polymer contains 6 atoms with altogether 12 valence orbitals (cf. Fig. 2 and Table IV). The chain is invariant with respect to the line group

$$L4_2/mcm = L4_2mc + (\hat{\sigma}_h \mid 0)L4_2mc \ .$$

The basic motif contains two atoms (Be_1 in the Γ_z position and H_1 in the Γ_v position) with 5 AO's ($\Phi_1^0, \ldots, \Phi_5^0$). The irreps of $L4_2mc$ are ${}_kA_0$, ${}_kA_2$, ${}_kB_0$, ${}_kB_2$ (one-dimensional), and ${}_kE_{1,-1}$ (two-dimensional). Using the LCAO SAB of $L4_2mc$, the 12-dimensional subspace $V(k)$ splits into $V(A_0)+V(A_2)+V(E_1)+V(E_{-1})$, where these three-dimensional subspaces correspond to ${}_kA_0$ and ${}_kA_2$, the first and second matrix columns of ${}_kE_{1,-1}$, respectively. In more detail, $V(A_0)$ and $V(A_2)$ are generated by projecting out Φ_1^0, Φ_2^0, and Φ_5^0 by $\hat{P}({}_kA_0)$ and $\hat{P}({}_kA_2)$, respectively; $V(E_1)$ is formed from Φ_3^0, Φ_4^0, and Φ_5^0 projected by $\hat{P}({}_kE_{1,-1})_{1,1}$. As expected from the twofold degeneracy, $\underline{S}(E_{-1}) = \underline{S}(E_1)$ if the basis of $V(E_{-1})$ is obtained via $\hat{P}({}_kE_{1,-1})_{2,1}$, so we need only three 3×3 Hermitian matrices $\underline{S}(A_0)$, $\underline{S}(A_2)$, and $\underline{S}(E_1)$. Their explicit form is given in Table IV. To simplify further the entries we have made use of the fact that $[\hat{\sigma}_v \mid 0]$ maps $\Phi_3^t, \Phi_4^t, \Phi_5^t, \Phi_{11}^t$ onto $\Phi_3^t, -\Phi_4^t, \Phi_5^t, \Phi_{12}^t$, respectively, so that

$$\begin{bmatrix} 0 & t \\ 3 & 4 \end{bmatrix} = \begin{bmatrix} 0 & t \\ 4 & 5 \end{bmatrix} = 0$$

and

$$\begin{bmatrix} 0 & t \\ 5 & 11 \end{bmatrix} = \begin{bmatrix} 0 & t \\ 5 & 12 \end{bmatrix} .$$

Similarly,

$$\begin{bmatrix} 0 & t \\ 3 & 5 \end{bmatrix} = -\begin{bmatrix} 0 & t \\ 3 & 6 \end{bmatrix}$$

and

$$\begin{bmatrix} 0 & t \\ 3 & 11 \end{bmatrix} = -\begin{bmatrix} 0 & t \\ 3 & 12 \end{bmatrix}$$

in view of $[\hat{C}_2 \mid 0]$: $\Phi_3^t \rightarrow -\Phi_3^t$, $\Phi_5^t \rightarrow \Phi_6^t$, $\Phi_{11}^t \rightarrow \Phi_{12}^t$. The forms of the blocks of $\underline{H}(k)$ are completely analogous; one just needs to replace

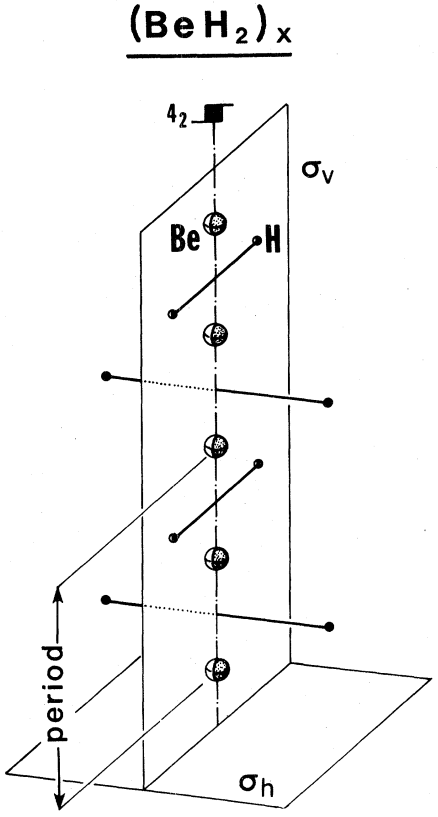

FIG. 2. Geometrical representation of $(BeH_2)_x$ model chain. Line-group symmetry is $L\,4_2/mcm$.

$$\begin{bmatrix} 0 & t \\ \mu & \nu \end{bmatrix}$$

by

$$\begin{bmatrix} 0 & & t \\ \mu & \hat{H} & \nu \end{bmatrix} .$$

Out of $\left(\begin{smallmatrix} 0 \\ \mu \end{smallmatrix} \middle| \begin{smallmatrix} t \\ \nu \end{smallmatrix}\right)$, $\mu,\nu=1,2,\ldots,12$, the following integrals are found to be redundant [cf. item (ii) of Sec. II G for the discussion of cases (1)—(3)]. For case (1),

$$\begin{bmatrix} 0 & t \\ \mu & \nu \end{bmatrix} \text{ for } \mu=6,7,\ldots,12 .$$

For case (2),

$$\begin{bmatrix} 0 & t \\ 1 & 3 \end{bmatrix}, \begin{bmatrix} 0 & t \\ 1 & 4 \end{bmatrix}, \begin{bmatrix} 0 & t \\ 1 & 9 \end{bmatrix}, \begin{bmatrix} 0 & t \\ 1 & 10 \end{bmatrix},$$
$$\begin{bmatrix} 0 & t \\ 2 & 3 \end{bmatrix}, \begin{bmatrix} 0 & t \\ 2 & 4 \end{bmatrix}, \begin{bmatrix} 0 & t \\ 2 & 9 \end{bmatrix}, \begin{bmatrix} 0 & t \\ 2 & 10 \end{bmatrix},$$
$$\begin{bmatrix} 0 & t \\ 3 & 7 \end{bmatrix}, \begin{bmatrix} 0 & t \\ 3 & 8 \end{bmatrix}, \begin{bmatrix} 0 & t \\ 4 & 7 \end{bmatrix}, \begin{bmatrix} 0 & t \\ 4 & 8 \end{bmatrix} .$$

For case (3),

$$\begin{bmatrix} 0 & t \\ 2 & 7 \end{bmatrix}, \begin{bmatrix} 0 & t \\ 4 & 9 \end{bmatrix}, \begin{bmatrix} 0 & t \\ 5 & 7 \end{bmatrix}, \begin{bmatrix} 0 & t \\ 5 & 8 \end{bmatrix}, \begin{bmatrix} 0 & t \\ 5 & 9 \end{bmatrix} .$$

To be completely specific, let us retain only the nearest-neighbor interactions. In the traditional approach, one must compute 66 overlap integrals; we reduce these to only 4, viz.,

$$\begin{bmatrix} 0 & 0 \\ 1 & 5 \end{bmatrix}, \begin{bmatrix} 0 & 0 \\ 2 & 5 \end{bmatrix}, \begin{bmatrix} 0 & 0 \\ 3 & 5 \end{bmatrix}, \begin{bmatrix} 0 & 0 \\ 5 & 6 \end{bmatrix} .$$

If we include the next-nearest neighbors, the 92 integrals reduce to 9; one needs also

$$\begin{bmatrix} 0 & 0 \\ 1 & 7 \end{bmatrix}, \begin{bmatrix} 0 & 0 \\ 1 & 8 \end{bmatrix}, \begin{bmatrix} 0 & 0 \\ 2 & 8 \end{bmatrix},$$
$$\begin{bmatrix} 0 & 0 \\ 3 & 10 \end{bmatrix}, \begin{bmatrix} 0 & 0 \\ 5 & 11 \end{bmatrix} .$$

Hence the savings of computation are remarkable.

B. Symmetry analysis of the band structure

The band structure of the $(BeH_2)_x$ polymer, calculated within the extended-Hückel crystalline orbital (EHCO) method, is presented in Fig. 3. A reasonable overall agreement is found with the *ab initio* results.[13,14]

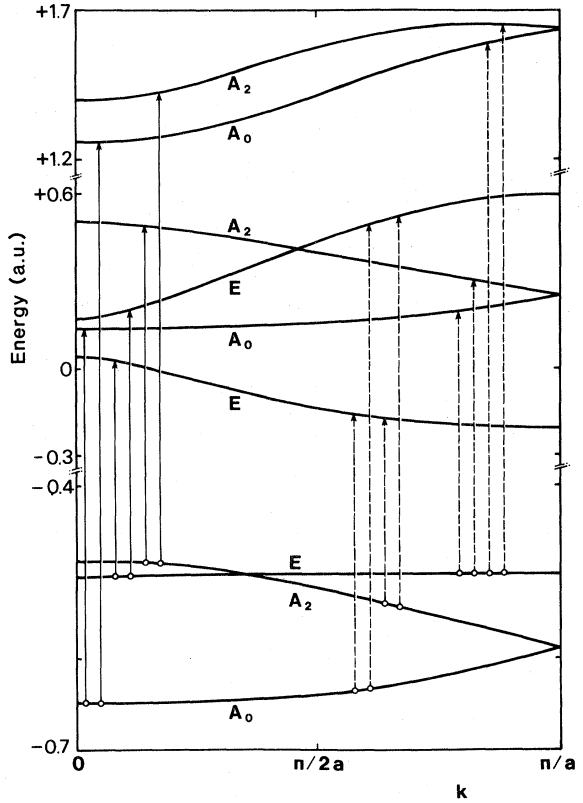

FIG. 3. Extended-Hückel energy band structure of $(BeH_2)_x$ polymer. The three E bands are twofold degenerate throughout the Brillouin zone. Vertical arrows indicate the symmetry-allowed transitions induced by absorption of light polarized in a plane containing the chain axis, for the perpendicular (——) and parallel (— — —) incidence, respectively.

TABLE V. Compatibility relations among the irreps of $L4_2/mcm$ at $k=0$ and π/a and the irreps of $L4_2mc$ for $0 \le k \le \pi/a$. The superscripts $\pm$ distinguish the irreps even and odd with respect to $(\hat{\sigma}_h \mid 0)$.

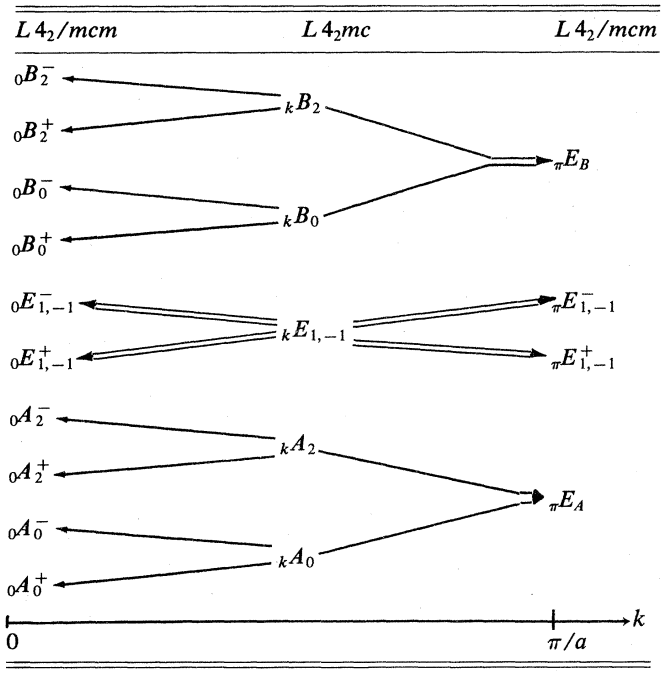

To each band we have assigned a symmetry label; i.e., the (abbreviated) symbol of the irrep of $L4_2mc$ according to which the corresponding one-electron states transform. In view of the results of Sec. III A we see (contrary to Ref. 14) that A_0 and A_2 states are linear combinations of $1s$(H), $2s$(Be), and $2p_z$(Be) orbitals and that the degenerate E states are made out of $1s$(H), $2p_x$(Be), and $2p_y$(Be) orbitals.

As a logical check of the obtained band structure, we can utilize the symmetry labels to analyze band touchings and slopes at the Brillouin-zone center and boundaries. The compatibility relations (cf. Table V) indeed indicate that the A_0 and A_2 bands should remain coupled when $k \to \pi/a$. In view of $\epsilon(k)=\epsilon(-k)$—as follows from σ_h symmetry and/or time-reversal symmetry—one has

$$\left.\frac{d\epsilon}{dk}\right|_{k=0} = 0$$

for each band and

$$\left.\frac{d\epsilon}{dk}\right|_{k=\pi/a} = 0$$

for the E bands. Finally,

$$\left.\frac{d\epsilon(A_0)}{dk}\right|_{k=\pi/a} = -\left.\frac{d\epsilon(A_2)}{dk}\right|_{k=\pi/a} \neq 0$$

for the A_0 and A_2 bands that touch at $k=\pi/a$. This can be easily seen if one observes that ${}_{k'}A_0 \equiv {}_kA_2$ for $k'=k+2\pi/a$, so that two bands $\epsilon({}_kA_0)$ and $\epsilon({}_kA_2)$—which are smooth and periodic in the Jones zone (i.e., twice the original Brillouin zone)—cross and reverse at $k=\pi/a$.

C. Selection rules

The symmetry labels are also useful in discussion of different processes in which the polymer may be involved; specifically, they allow one to derive easily the corresponding selection rules.[8,15] Let us, for example, consider direct optical absorption of a photon propagating along the x axis and polarized in the xz plane (the coordinate system is oriented as in Fig. 2). Taking for the moment only the $L4_2$ subgroup into account, we see that the transition is forbidden unless $\Delta m=0$, i.e., the allowed transitions are ${}_kA_{-1} \to {}_kA_{-1}$, ${}_kA_0 \to {}_kA_0$, ${}_kA_1 \to {}_kA_1$, ${}_kA_2 \to {}_kA_2$. Adding $(\hat{\sigma}_v \mid 0)$ now we enlarge the line group onto $L4_2mc$, with the effect that the ${}_kA_{-1}$ and the ${}_kA_1$ states become degenerate at the same time so that the selection rules are ${}_kA_0 \to {}_kA_0$, ${}_kE_{1,-1} \to {}_kE_{1,-1}$, ${}_kA_2 \to {}_kA_2$. Note that the energy defines mixed rather than pure states in the case of degeneracy; for the same reason the above-mentioned rules reduce at $k=\pi/a$ to ${}_\pi E_A \to {}_\pi E_A$, ${}_\pi E_{1,-1} \to {}_\pi E_{1,-1}$. On the other hand, if a beam of light of right circular polarization is directed along the z axis, $L4_2$ allows transitions with $\Delta m=+1$, i.e., ${}_kA_{-1} \to {}_kA_0$, ${}_kA_0 \to {}_kA_1$, ${}_kA_1 \to {}_kA_2$, ${}_kA_2 \to {}_kA_{-1}$ so that for $L4_2mc$ one obtains the following rules:

$${}_kA_0 \to {}_kE_{1,-1},\ {}_kA_2 \to {}_kE_{1,-1},\ {}_kE_{1,-1} \to {}_kA_0 \text{ or } {}_kA_2\ .$$

For the left circular polarization one has $\Delta m=-1$, but the final list of the transitions allowed by $L4_2mc$ is identical to that given above, as indeed expected for nonchiral (auto-enantiomorphic) chains such as the one under consideration. Finally, the same rules must apply also to a beam incident along the z axis and polarized in the xz (or any other vertical) plane; the rule for $L4_2$ is $\Delta m=\pm 1$ in this case. The first two cases are illustrated in Fig. 3, where the allowed direct optical transitions are represented by vertical arrows. It suggests that remarkable anisotropy and dichroism for the absorption of polarized light should be expected in $(BeH_2)_x$—of course, for a reasonably perfect sample.

IV. EXAMPLE: ALL-VALENCE-ELECTRON APPROACH TO TETRACYANOPLATINATE CHAIN

Let us consider now our second example, the $[Pt(CN)_4^{2-}]_x$ chain (CP in what follows) represented in Fig. 4. Compounds containing such chains have attracted much attention recently; $K_2[Pt(CN)_4]Br_{0.3}\cdot 3H_2O$ and its chloro analog are in fact the model systems for studying some phenomena (Peierls transitions, etc.) pertinent to quasi-1D conductors.

In view of detailed discussions in the preceding section, for the CP chain we give only the final results. Let us just note that larger format (84×84) of this eigenproblem enhances the relevance of symmetry arguments: They reduce a difficult numerical task to a moderate task.

The *translational repeat unit* of CP contains 18 atoms (two Pt, eight C, and eight N atoms), with 84 valence orbitals altogether ($5s,5p,5d,6s$ for Pt, $2s,2p$ for C, and $2s,2p$ for N). The *line group* of CP is

$$L8_4/mcm = L8_4mc + (\hat{\sigma}_h \mid 0)L8_4mc\ .$$

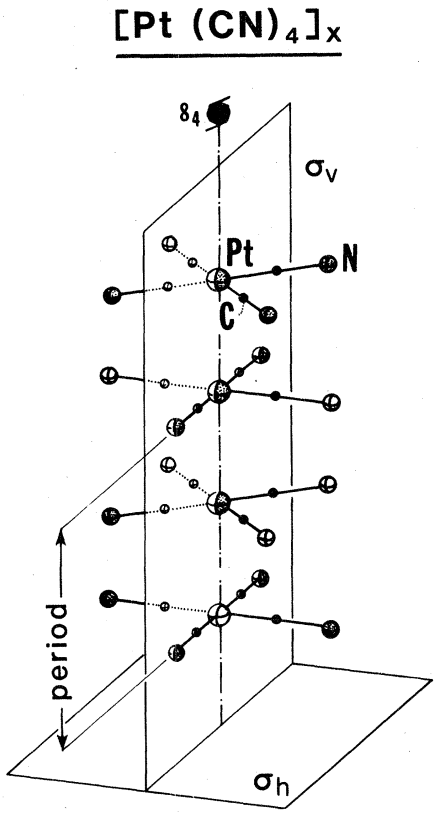

FIG. 4. Geometrical representation of $[Pt(CN)_4]_x$ model chain. Line-group symmetry is $L\,8_4/mcm$.

The *irreps* of $L\,8_4mc$ are ${}_kA_0$, ${}_kA_4$, ${}_kB_0$, ${}_kB_4$ (one-dimensional) and ${}_kE_{1,-1}$, ${}_kE_{2,-2}$, ${}_kE_{3,-3}$ (two-dimensional). The *basic motif* contains three atoms (Pt in the Γ_z position and C and N in the Γ_v position) with 18 AO's.

The formulas given in Table IX for the Γ_z graph and in Table X for the Γ_v graph enable one to write down immediately the complete LCAO SAB for the CP chain; one only needs to select, for each irrep ${}_k\underline{D}^{\alpha}$ of $L\,8_4mc$, the AO's belonging to the (zeroth) basic motif that contribute to the subspace $V({}_k\underline{D})$. This is accomplished in Table VI.

A. Block-diagonalization of $\underline{S}(k)$ and $\underline{H}(k)$

As follows from Table V, in the SAB formulation the eigenproblem of CP block-diagonalizes:

$$V(k)=V(A_0)+V(A_4)+V(B_0)+V(B_4)+2V(E_1)+2V(E_2)+2V(E_3)\,,$$

where $\dim V(k)=84$, $\dim V(B)=2$, and $\dim V(A)=\dim V(E)=10$; $2V(E_1)$ means that the $\underline{S}(E_1)$ block appears twice in $\underline{S}(k)$, etc. Therefore instead of an 84×84 matrix we must diagonalize five 10×10 blocks and two 2×2 blocks; in view of the roughly N^3 dependence of diagonalization complexity, the latter task is 2 orders of magnitude easier.

B. Reduction in the number of integrals

As an illustration, let us consider the CP chain in the approximation in which the integrals

$$\begin{pmatrix}0\,|\,t\\ \mu\,|\,\nu\end{pmatrix}\,,\quad \begin{pmatrix}0\,|\,\hat{H}\,|\,t\\ \mu\,|\,\nu\end{pmatrix}$$

are neglected unless the atoms involved belong to the same planar $Pt(CN)_4$ complex or to the neighboring complexes. In the calculation scheme utilizing only translational periodicity, one must calculate 6237 overlap integrals; further symmetry arguments reduce the number to only 257, i.e., for more than 24 times.

C. Band degeneracies, touchings, and slopes

The $E_{1,-1}$, $E_{2,-2}$, and $E_{3,-3}$ bands are twofold degenerate throughout the Brillouin zone. At the Brillouin-zone edge $k=\pi/a$, the A_0 bands remain coupled with the A_4 bands as do the B_0 and B_4 bands and the $E_{1,-1}$ and $E_{3,-3}$ bands. Note that in the last case we obtain fourfold degeneracy at the zone boundary; for more details see Table VII. The slopes at the center and at the edges of the Brillouin zone are the following:

TABLE VI. AO's from the (zeroth) basic motif of the CP chain which contribute to the subspace of the specified irrep of $L\,8_4mc$. The symmetry-adapted LCAO's are obtained when the AO's of Pt (given in the left-hand column below) are substituted into the formulas given in Table IX, and the AO's of C and N (the right-hand column) into those of Table X.

Subspace	Atomic orbitals	
	Pt	C,N
$V(A_0)$, $V(A_4)$	$5s$, $5p_z$, $5d_{z^2}$, $6s$	$2s$(C), $2p_z$(C), $2p_x$(C)
		$2s$(N), $2p_z$(N), $2p_x$(N)
$V(B_0)$, $V(B_4)$		$2p_y$(C), $2p_y$(N)
		$2s$(C), $2p_z$(C), $2p_x$(C), $2p_y$(C)
$V(E_1)$	$5p_x$, $5d_{xz}$	$2s$(N), $2p_z$(N), $2p_x$(N), $2p_y$(N)
		$2s$(C), $2p_z$(C), $2p_x$(C), $2p_y$(C)
$V(E_2)$, $V(E_3)$	$5d_{x^2-y^2}$, $5d_{xy}$	$2s$(N), $2p_z$(N), $2p_x$(N), $2p_y$(N)

TABLE VII. Compatibility relations among the irreps of $L\,8_4/mcm$ at $k=0$ and π/a and the irreps of $L\,8_4mc$ at $0\leq k<\pi/a$; cf. also Table V.

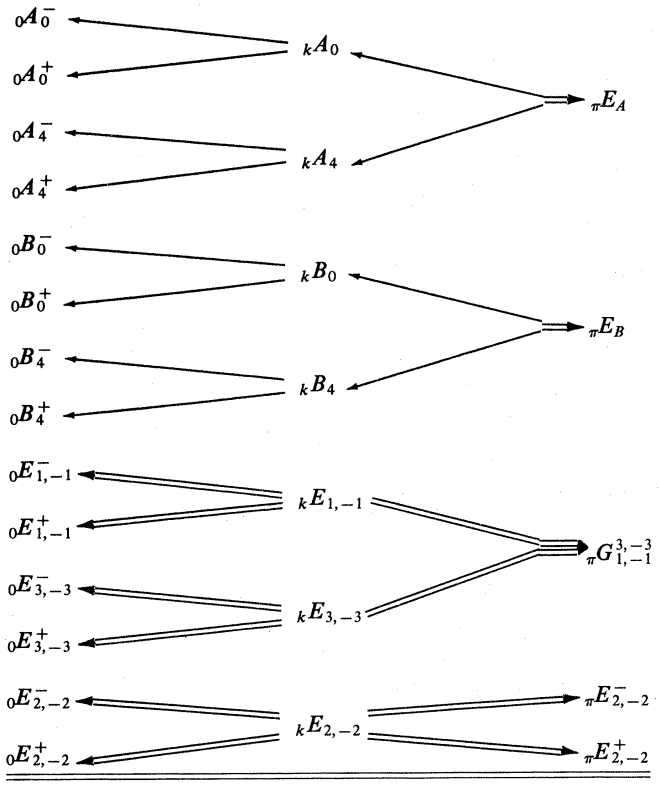

$$\left.\frac{d\epsilon}{dk}\right|_{k=0}=0$$

for each band,

$$\left.\frac{d\epsilon}{dk}\right|_{k=\pi/a}=0$$

for the $E_{2,-2}$ bands, and

$$\left.\frac{d\epsilon}{dk}\right|_{k=\pi/a}=-\left.\frac{d\epsilon'}{dk}\right|_{k=\pi/a}$$

for each pair $\{\epsilon(k),\epsilon'(k)\}$ of bands that cross at $k=\pi/a$, viz., for $\{\epsilon_{A_0}(k),\epsilon_{A_4}(k)\}$, $\{\epsilon_{B_0}(k),\epsilon_{B_4}(k)\}$, and $\{\epsilon_{E_1}(k),\epsilon_{E_3}(k)\}$.

D. Selection rules for direct optical absorption

In analogy to the results of Sec. III G we find the transitions between the states bearing the same labels—i.e., $_kA_0\rightarrow{}_kA_0,\ldots,{}_kE_3\rightarrow{}_kE_3$—allowed for the perpendicular incidence of light polarized along the chain axis. The selection rules for the parallel incidence are the following:

$$\left.\begin{matrix}A_0\\B_0\end{matrix}\right\}\rightarrow E_1,\quad\left.\begin{matrix}A_4\\B_4\end{matrix}\right\}\rightarrow E_3\ ,$$

$$E_1\rightarrow\begin{Bmatrix}E_2\\A_0,\\B_0\end{Bmatrix}\quad E_2\rightarrow\begin{Bmatrix}E_1\\E_3\end{Bmatrix}\ ,\quad E_3\rightarrow\begin{Bmatrix}E_2\\A_4\\B_4\end{Bmatrix}.$$

For $k=\pi/a$, the above rules degenerate into $E\rightarrow G$, $G\rightarrow E$, where E stands for $_\pi E_A$, $_\pi E_B$, or $_\pi E_{2,-2}^{\pm}$ and G for $_\pi G_{1,-1}^{3,-3}$, etc.

E. Crystal-field splitting

In view of the high symmetry of the CP chain, which includes a noncrystallographic 8_4 screw axis, it is interesting here to examine the effects of a crystalline environment. A single CP chain is invariant with respect to $(\hat{C}_8\,|\,\frac{1}{2})$, $(\hat{C}_4\,|\,0)$, $(\hat{C}_8^3\,|\,\frac{1}{2})$, $(\hat{C}_2\,|\,0)$, $(\hat{C}_8^5\,|\,\frac{1}{2})$, $(\hat{C}_4^3\,|\,0)$, $(\hat{C}_8^7\,|\,\frac{1}{2}),\ldots$, but when similar chains are packed into a crystal, the whole structure can at best be invariant with respect to $(\hat{C}_4\,|\,0),(\hat{C}_2\,|\,0),(\hat{C}_4^3\,|\,0),\ldots$. The $Pt(CN)_4$ chains are indeed found[10] in crystals of $I4/mcm$ space group symmetry, e.g., in $Cs_2[Pt(CN)_4]Cl_{0.30}$, $Rb_2[Pt(CN)_4](FHF)_{0.40}$, and $Cs_2[Pt(CN)_4](FHF)_{0.39}$, the latter one having remarkable $\sigma_{||}\sim 2000\ \Omega^{-1}\,cm^{-1}$. Thus we arrive at the problem of reduction of the irreducible representations $_k\underline{D}^{\alpha}(L\,8_4mc\downarrow L\,4mm)$, i.e., the irreps of the $L\,8_4mc$ line group restricted to its proper subgroup $L\,4mm$. The principal consequences are splitting each twofold degenerate $E_{2,-2}$ band into a pair of nondegenerate A_2 bands and eliminating all band touchings at $k=\pi/a$; for more de-

TABLE VIII. Effects of symmetry lowering from $L\,8_4/mcm$ onto $L\,4/mmm$. For the Brillouin zone center, let $k=0$ in the upper part of the table and add the $\pm$ superscript to each of the irreps.

$L\,8_4mc$	$_kA_0$	$_kA_4$	$_kB_0$	$_kB_4$	$_kE_{1,-1}$	$_kE_{2,-2}$	$_kE_{3,-3}$
$L\,4mm$	$_kA_0$	$_kA_0$	$_kB_0$	$_kB_0$	$_kE_{1,-1}$	$_kA_2\oplus{}_kA_2$	$_kE_{1,-1}$
$L\,8_4/mcm$	$_\pi E_A$	$_\pi E_B$	$_\pi E_{2,-2}^{\pm}$	$_\pi G_{1,-1}^{3,-3}$			
$L\,4/mmm$	$_\pi A_0^+\oplus{}_\pi A_0^-$	$_\pi B_0^+\oplus{}_\pi B_0^-$	$_\pi A_2^{\pm}\oplus{}_\pi A_2^{\pm}$	$_\pi E_{1,-1}^+\oplus{}_\pi E_{1,-1}^+$			

TABLE IX. LCAO SAB for the Γ_z graph (containing points on the z axis) of $L(2q)_q mc$, $q=1,2,\ldots$. The initial AO $\Phi_\lambda^{m_z}$ is centered at $\vec{R}=Z\vec{e}_z$; the subscript λ stands for 0 if $m_z=0$ and for + or − if $m_z=1,2\ldots$. The translation period is denoted by a; $t=0,\pm1,\ldots$, but in view of the cyclic Born–von Kármán boundary conditions it takes on only N inequivalent values. The abbreviation $\Phi_\lambda^{m_z}(t)$ means $\Phi_\lambda^{m_z}[x\vec{e}_x+y\vec{e}_y+(z-Z-ta)\vec{e}_z]$ and analogously $\Phi_\lambda^{m_z}(t+\frac{1}{2})=\Phi_\lambda^{m_z}[x\vec{e}_x+y\vec{e}_y+(z-Z-ta-a/2)\vec{e}_z]$; $\gamma=\exp(ika/2)$, $-\pi/a<k\le\pi/a$, and $m=1,2,\ldots,q-1$. For given q and m_z, one and only one of the following four possibilities is satisfied: (i) $m_z=hq$, $h=1,2,\ldots$, (ii) $\mathrm{Fr}(m_z/q)=\frac{1}{2}$ and $m=q/2$, (iii) $m=-z+(h+1)q$, or (iv) $m=m_z-hp$, where $h=\mathrm{Int}(m_z/q)$. Here $\mathrm{Int}(x)$ and $\mathrm{Fr}(x)$ denote the integral and the fractional part of x, respectively. SALC_1 corresponds to the first column of the representation considered. For the ${}_kE_{m,-m}$ irreps, SALC_2 is obtained by replacing $\Phi_-^{m_z}$ by $-\Phi_-^{m_z}$ in the above expressions for SALC_1.

irrep	AO projected	SALC_1
${}_kA_0$	Φ_0	$\frac{1}{2N}\sum_t \exp(-ikta)[\Phi_0(t)+\gamma\Phi_0(t+\frac{1}{2})]$
	$\Phi_+^{m_z}$ if $m_z=hq$	$\frac{1}{2N}\sum_t \exp(-ikta)[\Phi_+^{m_z}(t)+\gamma(-1)^h\Phi_+^{m_z}(t+\frac{1}{2})]$
${}_kA_q$	same as for ${}_kA_0$ but replace γ by $-\gamma$	
${}_kB_0$	$\Phi_-^{m_z}$ if $m_z=h_q$	$\frac{1}{2n}\sum \exp(-ikta)[\Phi_-^{m_z}(t)+\gamma(-1)^h\Phi_-^{m_z}(t+\frac{1}{2})]$
${}_kB_q$	same as for ${}_kB_0$ but replace γ by $-\gamma$	
${}_kE_{m,-m}$ with $m=q/2$	$\Phi_+^{m_z}$ if $\mathrm{Fr}(m_z/q)=\frac{1}{2}$	$\frac{1}{2N}\sum_t \exp(-ikta)[\Phi_+^{m_z}(t)-i\gamma(-1)^h\Phi_-^{m_z}(t+\frac{1}{2})]$
	$\Phi_-^{m_z}$ if $\mathrm{Fr}(m_z/q)=\frac{1}{2}$	$\frac{1}{2N}\sum_t \exp(-ikta)[\Phi_-^{m_z}(t)+i\gamma(-1)^h\Phi_+^{m_z}(t+\frac{1}{2})]$
${}_kE_{m,-m}$ with $m\neq q/2$	$\Phi_+^{m_z}$ if $m_z=-m+(h+1)q$	$\frac{1}{4N}\sum_t \exp(-ikta)\{[\Phi_+^{m_z}(t)+i\Phi_-^{m_z}(t)]-\gamma(-1)^h[\Phi_+^{m_z}(t+\frac{1}{2})+i\Phi_-^{m_z}(t+\frac{1}{2})]\}$
	$\Phi_+^{m_z}$ if $m_z=m+hq$	$\frac{1}{4N}\sum_t \exp(-ikta)\{[\Phi_+^{m_z}(t)-i\Phi_-^{m_z}(t)]+\gamma(-1)^h[\Phi_+^{m_z}(t+\frac{1}{2})-i\Phi_-^{m_z}(t+\frac{1}{2})]\}$

TABLE X. LCAO SAB for the Γ_v graph (containing points in the xz plane) of $L(2q)_q mc$, $q=1,2,\ldots$; the initial AO is $\Phi_\lambda^{m_z}=\Phi_\lambda^{m_z}[(x-X)\vec{e}_x+y\vec{e}_y+(z-Z)\vec{e}_z]$, centered at $R=X\vec{e}_z+Z\vec{e}_z$. The abbreviation ${}_kP_m\Phi_\lambda^{m_z}$ is defined in the first part of the table, where the $\hat{C}_n^s$ term is given as in Eqs. (2b) and (2c). In ${}_kP_m\Phi_\lambda^{m_z}$, $s=2r$ in the first term and $s=2r+1$ in the second. $\gamma=\exp(ika/2)$, $r=0,1,\ldots,q-1$ and $\alpha=\pi/q$; for λ, a, t, k, and m, see the caption of Table IX.

Definition of ${}_kP_m\Phi_\lambda^{m_z}$

$$
{}_kP_m\Phi_\lambda^{m_z}=\frac{1}{4qN}\sum_t\sum_{r=0}^{q-1}\exp(-ikta)\{\exp(-i2rm\alpha)\tilde{\Phi}_\lambda^{m_z}([x-\cos(2r\alpha)X]\vec{e}_x+\{y-\sin[(2r\alpha)X]\}\vec{e}_y+(z-Z-ta)\vec{e}_z)
$$
$$
+\gamma\exp[-i(2r+1)m\alpha]\tilde{\Phi}_\lambda^{m_z}(\{x-\cos[(2r+1)\alpha]X\}\vec{e}_x+\{y-\sin[(2r+1)\alpha]X\}\vec{e}_y
$$
$$
+(z-Z-ta-a/2)\vec{e}_z)\},\ \text{where}
$$

$$
\tilde{\Phi}_\lambda^{m_z}=\hat{C}_n^s\Phi_\lambda^{m_z}=\begin{cases}\Phi_0 & \text{if } m_z=\lambda=0\\ \cos(m_zs\alpha)\Phi_+^{m_z}+\sin(m_zs\alpha)\Phi_-^{m_z} & \text{if } \Phi_\lambda^{m_z}=\Phi_+^{m_z}\\ -\sin(m_zs\alpha)\Phi_+^{m_z}+\cos(m_zs\alpha)\Phi_-^{m_z} & \text{if } \Phi_\lambda^{m_z}=\Phi_-^{m_z}\end{cases}
$$

irrep	${}_kA_0$		${}_kA_q$		${}_kB_0$	${}_kB_q$	${}_kE_{m,-m}$		
AO	Φ_0	$\Phi_+^{m_z}$	Φ_0	$\Phi_+^{m_z}$	$\Phi_-^{m_z}$	$\Phi_-^{m_z}$	Φ_0	$\Phi_+^{m_z}$	$\Phi_-^{m_z}$
$SALC_1$	${}_kP_0\Phi_0$	${}_kP_0\Phi_+^{m_z}$	${}_kP_q\Phi_0$	${}_kP_q\Phi_+^{m_z}$	${}_kP_0\Phi_-^{m_z}$	${}_kP_q\Phi_-^{m_z}$	${}_kP_m\Phi_0$	${}_kP_m\Phi_+^{m_z}$	${}_kP_m\Phi_-^{m_z}$
$SALC_2$							${}_kP_{-m}\Phi_0$	${}_kP_{-m}\Phi_+^{m_z}$	$-{}_kP_{-m}\Phi_-^{m_z}$

TABLE XI. LCAO SAB for the Γ_a graph of $L(2q)_q mc$, $q=1,2,\ldots$. Here the initial AO, $\Phi_\lambda^{m_z}(1)=\Phi_\lambda^{m_z}(\vec{r}-\vec{R})$, is centered at an arbitrary asymmetric position $R=X\vec{e}_x+Y\vec{e}_y+Z\vec{e}_z$. Abbreviations for $\Phi_\lambda^{m_z}(2)$ and ${}_kP_m\Phi_\lambda^{m_z}(1)$ are given in the first part of the table. k, t, a, r, m, α, $\Phi_\lambda^{m_z}$, and γ have the same meaning as in Table X. For ${}_kP_m\Phi_\lambda^{m_z}(2)$, replace Y by $-Y$ in the expression below for ${}_kP_m\Phi_\lambda^{m_z}(1)$.

Definition of $\Phi_\lambda^{m_z}(2)$ and ${}_kP_m\Phi_\lambda^{m_z}(1)$

$$\Phi_\lambda^{m_z}(2)=\Phi_\lambda^{m_z}(\vec{r}-\sigma_v^1\vec{R})=\Phi_\lambda^{m_z}[(x-X)\vec{e}_x+(y+Y)\vec{e}_y+(z-Z)\vec{e}_z]$$

$$\begin{aligned}{}_kP_m\Phi_\lambda^{m_z}(1)=\frac{1}{4qN}\sum_t \exp(-ikta)\{&\exp(-i2rm\alpha)\tilde{\Phi}_\lambda^{m_z}\{[x-\cos(2r\alpha)X-\sin(2r\alpha)Y]\vec{e}_x+[y+\sin(2r\alpha)X-\cos(2r\alpha)Y]e_y+(z-Z-ta)\vec{e}_z\}\\&+\gamma\exp[-i(2r+1)m\alpha]\tilde{\Phi}_\lambda^{m_z}(\{x-\cos[(2r+1)\alpha]X-\sin[(2r+1)\alpha]Y\}\vec{e}_x\\&+\{y+\sin[(2r+1)\alpha]X-\cos[(2r+1)\alpha]Y\}\vec{e}_y+(z-Z-ta-a/2)\vec{e}_z)\}\end{aligned}$$

irrep	${}_kA_0$		
AO	$\Phi_0(1)$	$\Phi_+^{m_z}(1)$	$\Phi_-^{m_z}(1)$
$SALC_1$	$\frac{1}{2}{}_kP_0[\Phi_0(1)+\Phi_0(2)]$	$\frac{1}{2}{}_kP_0[\Phi_+^{m_z}(1)+\Phi_+^{m_z}(2)]$	$\frac{1}{2}{}_kP_0[\Phi_-^{m_z}(1)-\Phi_-^{m_z}(2)]$

irrep ${}_kA_q$: same as for ${}_kA_0$, but replace ${}_kP_0$ by ${}_kP_q$

irrep	${}_kB_0$		
AO	$\Phi_0(1)$	$\Phi_+^{m_z}(1)$	$\Phi_-^{m_z}(1)$
$SALC_1$	$\frac{1}{2}{}_kP_0[\Phi_0(1)-\Phi_0(2)]$	$\frac{1}{2}{}_kP_0[\Phi_+^{m_z}(1)-\Phi_+^{m_z}(2)]$	$\frac{1}{2}{}_kP_0[\Phi_-^{m_z}(1)+\Phi_-^{m_z}(2)]$

irrep ${}_kB_q$: same as for ${}_kB_0$, but replace ${}_kP_0$ by ${}_kP_q$

irrep	${}_kE_{m,-m}$					
AO	$\Phi_0(1)$	$\Phi_+^{m_z}(1)$	$\Phi_-^{m_z}(1)$	$\Phi_0(2)$	$\Phi_+^{m_z}(2)$	$\Phi_-^{m_z}(2)$
$SALC_1$	${}_kP_m\Phi_0(1)$	${}_kP_m\Phi_+^{m_z}(1)$	${}_kP_m\Phi_-^{m_z}(1)$	${}_kP_m\Phi_0(2)$	${}_kP_m\Phi_+^{m_z}(2)$	${}_kP_m\Phi_-^{m_z}(2)$
$SALC_2$	${}_kP_{-m}\Phi_0(2)$	${}_kP_{-m}\Phi_+^{m_z}(2)$	$-{}_kP_{-m}\Phi_-^{m_z}(2)$	${}_kP_{-m}\Phi_0(1)$	${}_kP_{-m}\Phi_+^{m_z}(1)$	$-{}_kP_{-m}\Phi_-^{m_z}(1)$

tails see Table VIII. Some other space groups ($P\bar{4}b2, P4mm, C2/c, P\bar{1}$) are also found[10] in compounds containing CP chains; these cases can be treated analogously.

ACKNOWLEDGMENTS

One of the authors (I.B.) would like to express his gratitude to the Department of Physics, University of California, Berkeley and to Professor Leo Falicov for hospitality and to the Council for International Exchange of Scholars (CIES) for a Fulbright fellowship. This work was supported in part by National Science Foundation Grant No. DMR-81-06494 and also made possible by visiting programs within Belgo-Yugoslav Scientific exchange agreements.

APPENDIX: LCAO SAB's FOR THE $L(2q)_q mc$ LINE GROUPS

The problem posed in Sec. II B—to construct and tabulate the symmetry-adapted LCAO's—is solved here for the selected family of line groups, $L(2q)_q mc$. After reproducing the irreps of $L(2q)_q mc$ (in Table III) for the reader's convenience, we give explicitly (in Tables IX–XI) the symmetry-adapted linear combinations (SALC) of the initial atomic orbitals for each graph, each irrep of $L(2q)_q mc$, and each type of AO. The tabulated SAB spans the whole variational space V and is linearly independent—for a given graph and irrep we omit the AO's that project onto zero or onto functions linearly dependent on those already tabulated.

---

*Permanent address: Institute of Physics, P.O. Box 57, 11000 Belgrade, Yugoslavia.

[1] *Highly Conducting One-Dimensional Solids,* edited by J. T. Devreese, R. P. Evrard, and V. E. van Doren (Plenum, New York, 1979); *Molecular Metals,* edited by W. E. Hatfield (Plenum, New York, 1979); *Conductive Polymers,* edited by R. B. Seymour (Plenum, New York, 1979); *Quasi One-Dimensional Conductors I* and *II,* Vols. 95 and 96 of *Lecture Notes in Physics,* edited by S. Barišić, A. Bjeliš, J. R. Cooper, and B. Leontić (Springer, Berlin, 1979); J. Mort, Adv. Phys. 29, 367 (1980); *The Physics and Chemistry of Low-Dimensional Solids,* edited by L. Alcácer (Reidel, Dordrecht, 1980); *Physics in One Dimension,* edited by J. Bernasconi and T. Schneider (Springer, Berlin, 1981).

[2] *Recent Advances in the Quantum Theory of Polymers,* Vol. 113 of *Lecture Notes in Physics,* edited by J.-M. André, J.-L. Brédas, J. Delhalle, J. Ladik, G. Leroy, and C. Moser (Springer, Berlin, 1980); J.-M. André, in *Advances in Quantum Chemistry,* edited by P. O. Löwdin (Academic, New York, 1980), Vol. 12, pp. 65–102.

[3] B. K. Vainshtein, Krystallografiya 4, 842 (1959); *Diffraction of X-Rays by Chain Molecules* (Elsevier, Amsterdam, 1966).

[4] M. Vujičić, I. Božović, and F. Herbut, J. Phys. A 10, 1271 (1977).

[5] A. Blumen and C. Merkel, Phys. Status Solidi B 83, 425 (1977); J. Ladik, in *Excited State in Quantum Chemistry,* edited by C. A. Nicolaides and D. R. Beck (Reidel, Dordrecht, 1978), p. 495.

[6] W. L. McCubbin, Chem. Phys. Lett. 8, 507 (1971); W. L. McCubbin, in *Electronic Structure of Polymers and Molecular Crystals,* edited by J.-M. André and J. Ladik (Plenum, London, 1975); W. Rhodes, J. Chem. Phys. 37, 2433 (1962).

[7] I. Božović, M. Vujičić, and F. Herbut, J. Phys. A 11, 2133 (1978); I. Božović and M. Vujičić, *ibid.* 14, 777 (1981); I. Božović and N. Božović, *ibid.* 14, 1825 (1981); I. Božović, *ibid.* 15, 2661 (1982).

[8] I. Božović, J. Delhalle, and M. Damnjanović, Int. J. Quant. Chem. 20, 1143 (1981).

[9] J. Brendel, E. M. Marlett, and L. M. Niebylski, Inorg. Chem. 17, 3589 (1978); K. Subba Rao and M. Srinivasan, Nucl. Technol. 49, 315 (1980).

[10] P. Day, in *The Physics and Chemistry of Low Dimensional Solids,* edited by L. Alcácer (Reidel, Dordrecht, 1980), p. 305; P. Day, in *Low-Dimensional Cooperative Phenomena,* edited by J. J. Keller (Plenum, New York, 1975), p. 191.

[11] M. Lax, *Symmetry Principles in Solid State and Molecular Physics* (Wiley, New York, 1974); H. W. Streitwolf, *Group Theory in Solid State Physics* (McDonald, London, 1971).

[12] S. Flodmark, Phys. Rev. 132, 1343 (1963); E. Blokker, J. Comp. Phys. 12, 471 (1973); S. Flodmark and R. O. Jansson, Physica (in press).

[13] A. Karpfen, Theor. Chim. Acta 50, 49 (1978).

[14] D. R. Armstrong, J. Jamieson, and P. G. Perkins, Theor. Chim. Acta. 51, 163 (1979).

[15] M. Damnjanović, I. Božović, and N. Božović, J. Phys. A 16, 3937 (1983).